UNIVERSITY OF LEEDS

Article:
Obuh, IE, Doychinov, V orcid.org/0000-0001-6730-0057, Steenson, DP et al. (3 more authors) (2018) Low-Cost Microfabrication for MEMS Switches and Varactors. IEEE Transactions on Components, Packaging and Manufacturing Technology, PP (99). pp. 1-9. ISSN 2156-3950

https://doi.org/10.1109/TCPMT.2018.2834865

IEEE Transactions on Components, Packaging, and Manufacturing Technology

Low-Cost Micro-Fabrication for MEMS Switches and Varactors

Journal:	*Transactions on Components, Packaging and Manufacturing Technology*
Manuscript ID	TCPMT-2017-513.R1
Manuscript topic:	ELECTRONICS MANUFACTURING
Date Submitted by the Author:	21-Feb-2018
Complete List of Authors:	Obuh, Isibor; University of Leeds, School of Electronic and Electrical Engineering Doychinov, Viktor; University of Leeds, Institute of Robotics, Autonomous Systems, and Sensing Steenson, David; University of Leeds, Electronic and Electrical Eng Akkaraekthalin, Prayoot; King Mongkut's University of Technology North Bangkok, Department of Electrical and Computer Engineering Robertson, Ian; University of Leeds, School of EEE Somjit, Nutapong; University of Leeds, Institute of Microwaves and Photonics
Keywords:	Microelectromechanical devices, Micromachining, Microwave devices

Low-Cost Micro-Fabrication for MEMS Switches and Varactors

Isibor E. Obuh, Student Member, IEEE, Viktor Doychinov, Member IEEE, David P. Steenson, Senior Member IEEE, Prayoot Akkaraekthalin, Member, IEEE, Ian D. Robertson, Fellow, IEEE, and Nutapong Somjit, Member IEEE

Abstract—This paper presents a low-cost micro-fabrication technique for manufacturing RF MEMS switches and varactors without intensive cleanroom environments. The fabrication process entails only laser micro-structuring technique, non-cleanroom micro-lithography, standard wet-bench and hot-film emboss of SU-8 and ADEX polymers. MEMS movable structures were fabricated out of 14-µm-thick Aluminum foils and suspended above coplanar-waveguide transmission lines, which were implemented on top of FR4 substrates, via 5-µm-thick SU-8 dielectric anchors. Both MEMS structures and FR4 substrate were integrated using micro-patterned polymers, developed by using dry-film ADEX and SU-8 polymers, for a composite assembly. An average fabrication yield of higher than 60% was achieved, calculated from ten fabrication attempts. The RF measurement results show that the RF MEMS devices fabricated by using the novel micro-fabrication process have good figure-of-merits, at much lower overall fabrication costs, as compared to the devices fabricated by conventional cleanroom process, enabling it as a very good micro-fabrication process for cost-effective rapid prototyping of MEMS.

Index Terms — Subtractive manufacturing, micro electromechanical systems (MEMS), rapid prototyping.

I. Introduction

Radio-frequency microelectromechanical systems (RF MEMS) are mostly fabricated by using cleanroom-based fabrication technology. Cleanroom fabrication techniques consist of intricate development cycles, which includes metal and dielectric film depositions, material etching and chemical processes. Cleanroom-based processes require well-controlled air-circulation, ventilation, and filtering systems with the ultimate goal to minimize contaminants that may interfere with the fabrication process [1]. These imperatives as well as the associated investment and operational costs, for cleanroom equipment and maintenance, ensure relatively steep budgets are required to manufacture MEMS structures. Cleanroom-based processes consist of substrate preparation, thin film metal and dielectric deposition, pattern etching, and membrane release methods [1]. Fabrication techniques examined in [2-5], employed these processes with variations in complexity, cost and estimated development timescales. In comparison, the techniques developed in this paper are non-clean room based, inexpensive, and achieve satisfactory yields with quicker turnaround times. In [2] a dimple shaped RF MEMS switch was fabricated on an alumina substrate using an eight step clean room based process. A combination of Physical Vapor Deposition (PVD) and Plasma-Enhanced Chemical Vapor Deposition (PECVD), as well as thermal evaporation, were used to deposit the conductive and dielectric layers that comprise an RF MEMS device. Materials used were TiW, Cr/Au, and SiO_2. MEMS features were defined using Reactive Ion Etching (RIE), O_2 plasma dry etching, and photolithography.

A similar procedure based on a four mask process was employed in [3], for an RF MEMS switch fabricated on a TMM4 PCB substrate. Conductive layers were formed from Ti/Cu, Au, and Cr/Au; whereas Si_3N_4, deposited by High-Density Inductively Coupled Plasma Chemical Vapor Deposition (HDICP CVD), was used as a dielectric layer. Features were defined using selective wet etching and resist removal using an acetone soak.

In [4], bonded silicon and glass wafers were used as substrates. Dielectric layers were formed of SiO_2 and Poly-Si, deposited by PECVD and Low-Pressure CVD (LPCVD) methods, respectively. Metal tracks were formed from Au, with RIE and ICP-RIE used to define CPW transmission lines and other necessary features. In addition, the bonding of the silicon and glass wafers was achieved using solutions of H_2O_2, H_2SO_4, and HF.

Research work in [5], aimed at reducing clean room based fabrication costs, explored a springless switch design fabricated with a three wafer assembly, consisting of a glass slide, a Rogers RO4003 board, and a silicon wafer. Metal in the form of an Au/Cr layer was deposited on the glass slide using thermal evaporation, and feature patterning was achieved using photolithography with dry film resist. Dielectric layers were formed out of Ta_2O_5.

This work has been supported in part by the Engineering and Physical Sciences Research Council (EPSRC) under Grant EP/N010523/1, the Thailand Research Fund through the TRF Senior Research Scholar Program with Grant No. RTA6080008, the Royal Golden Jubilee Ph.D. Program with Grant No.PHD/0093/2557.

I. E. Obuh, V. Doychinov, D. P. Steenson, I. D. Robertson and N. Somjit are with the department of Electronic and Electrical Engineering, University of Leeds, United Kingdome, LS2 9JT (e-mail: el12ieo@leeds.ac.uk; V.O.Doychinov@leeds.ac.uk; D.P.Steenson@leeds.ac.uk; I.D.Robertson@leeds.ac.uk; N.Somjit@leeds.ac.uk.

P. Akkaraekthalin is with the Department of Electrical and Computer Engineering, Faculty of Engineering, King Mongkut's University of Technology North Bangkok, Bangsue, Bangkok, 10800, Thailand (e-mail: prayoot@kmutnb.ac.th).

Recent efforts aimed at cost reduction for MEMS micro-fabrication, involved polymer based materials employed as both dielectric and adhesive bonds, with layer transfer manufactured by volume stamping or spin coating [6]. In addition, research interests in alternatives to traditional cleanroom based substrates were reported with intensive investigations into usage of ceramics and fiberglass-based PCB substrates [3, 6-10]. Photosensitive Benzocyclobutene (BCB), SU-8, fluorinated poly (Arlene ethers) and fluoropolymer cyclized perfluoro (CPFP) polymers were experimented as low-cost replacement for inorganic films in MEMS fabrications, with patterning of deposited polymer film coated by photolithography process [6], [11].

As an example, PCB MEMs varactors fabricated using cleanroom technologies, were reported in [7], with deep-reactive ion etching (DRIE) process employed in MEMS Kapton membrane fabrication. Benzocyclobutene (BCB) was employed as the dielectric layer for etched coplanar waveguide (CPW) transmission lines. The dielectric layer for PCB MEMS switches reported in [8] was fabricated with an inductively coupled plasma (ICP) reactor. Wet etching was employed for structuring of the CPW with additional plating at the switch position. Research studies involving PCB-based MEMS fabrication processes have been reported in [3], [8-10], and are intensively cleanroom-based, with the accompanying complexity and production cost earlier observed.

This paper presents a novel micro-fabrication method, without intensive cleanroom manufacturing techniques and the associated mitigating equipment and processing costs. Laser micro-structuring processes are employed to fabricate MEMS deflecting membranes, microlithography masks, and for etching the transmission lines on the substrates. In addition, an optimized hybrid manufacturing process of the wet bench and dry-film emboss process for both SU-8 and ADEX polymers deposition was investigated and optimized for the RF MEMS integration and bonding process. In this work, RF MEMS switches and varactors operating up to 3 GHz were manufactured, for demonstrating purpose, by using the previously mentioned micro-fabrication techniques. The non-cleanroom fabrication methods employed, stems from a focus on exploring cost-effective alternatives to realizing RF MEMs structures, ensures sufficient bonding, with minimal packaging requirement to additional RF devices on PCB. The fabrication technique also resulted in reasonable yields of 60% with simple fabrication development cycles. The main challenge and limiting factor to achieving higher yields is controlling the environment outside of a clean room, e.g. ambient light level and dust and particle contamination. However, the use of a fume cupboard with a guard screen, in combination with blue light filters, were found to be sufficient for this quick, low-cost process.

II. MEMS Switches and Varactor Design

A 3D model of the MEMS switch design used to demonstrate the fabrication method presented in this paper, in both of its operational states, is shown in Fig. 1. The up-state position is depicted in Fig. 1 (a), also referred to as the zero bias or OFF state; the down-state is shown in Fig. 1 (b), which is the bias condition or ON state. The MEMS switch consists of a coplanar waveguide transmission line with signal conductor width of 460 µm and a 95-µm gap, up to the switch location, where it widens to 340 µm. A 14-µm-thick, H-shaped, Aluminum bridge membrane is suspended, 6 µm, above the coplanar waveguide, and is attached at both anchor ends by ADEX epoxy polymers. In addition, there are two polymer posts at the anchors to electrically isolate the MEMS aluminum bridge from the ground of the CPW. Then, a 1-µm SU-8 layer provides similar electrical decoupling fabricated on top of the center signal conductor.

The device parameters derived from the equivalent model of a MEMS switch reported in [12], alongside the capacitance ratio of the switch in both states examined in [13, 14] were optimized with fabrication limitations and project objectives

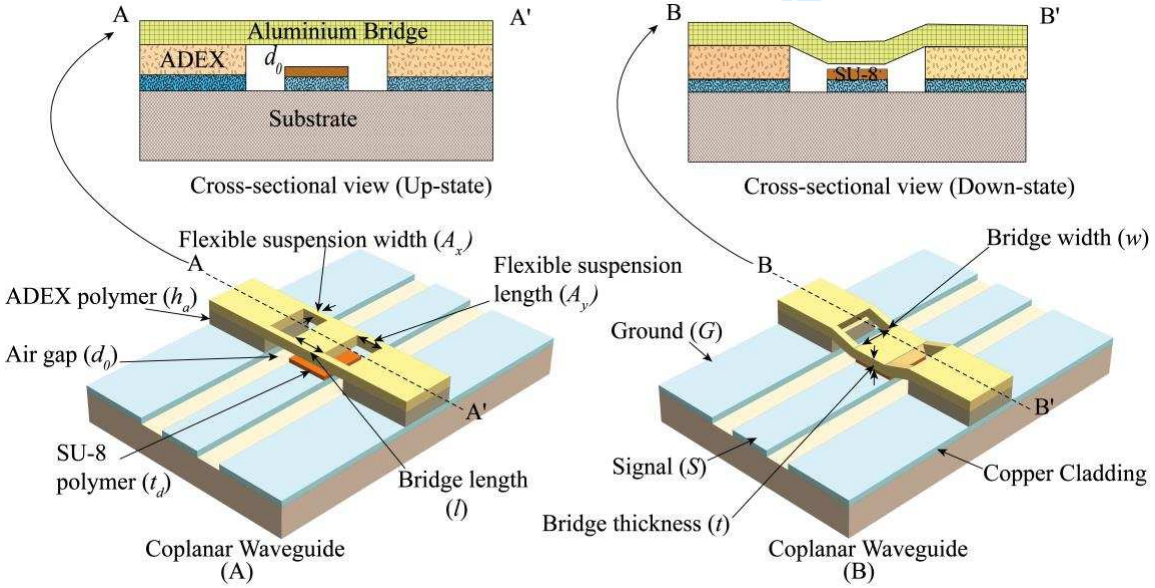

Fig. 1. 3D model and cross-sectional view of MEMS switches and varactors for both Upstate and Downstate positions.

as constraints.

The design of the RF MEMS switch and varactor begins with determining the dimensions of the CPW transmission line, i.e. the gap G and signal line width S, which play an important roles in the devices' signal loss and bandwidth response and determine the switch and varactor bridge length. The gap and signal line width were determined to be 340 µm and 460 µm, respectively, for a standard line impedance Z_0 of 50 Ω. The design of the CPW line was performed using Keysight's Advanced Design System (ADS)[1] for a CPW line on a low-cost FR4 substrate, and its performance verified using the commercial 3D EM simulator Ansys HFSS[2].

An important parameter of both the RF MEMS switch and varactor is their capacitance ratio, which determines the isolation between the two states (ON and OFF) of the switch and the limits of the variable shunt capacitance presented by the varactor. The capacitance ratio is given by [15]:

$$C_r = \frac{C_d}{C_u} = \frac{{}^{\varepsilon_0 \varepsilon_r A}/_{t_d}}{\frac{\varepsilon_0 A}{d_0 + \frac{t_d}{\varepsilon_r}} + C_f} \quad (1)$$

Where ε_r is the relative permittivity of the SU8 dielectric film on the signal line of the switch area, t_d is the SU8 dielectric film thickness, A is the capacitive area of the bridge, d_0 is the bridge height, C_d, C_f and C_u, are the down state, fringe and up state capacitances, respectively. For the RF MEMS switch and varactor used to demonstrate the novel fabrication process, C_r values of 50 and 4 were chosen, respectively. The corresponding bridge width w can then be obtained from the capacitive area A which is defined as $S \times w$.

The DC actuation voltage V_a, which is the control signal that is applied to the RF MEMS switch and varactor, can then be determined by [15]:

$$V_a = \sqrt{\frac{8k}{27\varepsilon_0 S w} d_0^3} \quad (2)$$

Where k is the spring constant of the bridge, ε_0 is the permittivity of vacuum, w the bridge width, S the signal line width, and d_0 is the bridge height. As observed from (2), to realize an RF MEMS switch with low actuation voltage, a low spring constant k bridge design is required, and additionally the bridge height should be small and the capacitance area large. Two bridge topologies with available analytical expressions for k were chosen and used for the switch and varactor in this paper. These are fixed to fixed [16] and crab leg flexure [17], respectively. With capacitive bridge areas and ratios derived, the symbolic solver tool in Matlab[3] was used to obtain the design values for the RF MEMS switch and varactor. Table I provides a summary of these parameters.

TABLE I
DIMENSIONS OF RF MEMS DEVICES AND MATERIAL PARAMETERS

Symbol	Geometry and material parameter	Switch	Varactor
E	Young Modulus of Al	70 GPa	70 GPa
l	Bridge length	800 µm	450 µm
w	Bridge width	600 µm	700 µm
t	Bridge thickness	14 µm	14 µm
d_0	Bridge height	6 µm	2 µm
A_x	Suspension width	100 µm	100 µm
A_y	Suspension length	140 µm	140 µm
t_d	Dielectric height	1 µm	1 µm
C_r	Capacitance ratio	50	4
V_a	Actuation Voltage	85	15

Laser micromachining, wet bench and dry film emboss processes were adopted in line with project objectives to implement these RF MEMS switches and varactors. These fabrication processes were primarily developed and optimized on PCB, ensuring prospects for integration of additional RF devices and Monolithic Microwave Integrated Circuits (MMIC) [8].

III. Fabrication Process

The MEMS switch and varactor bridge structures are fabricated from high-purity 14-µm thick Aluminum foils, mounted 6 µm above a CPW transmission line. These lines were etched on a rigid, 1.524-mm thick, low-cost, thermoset laminate FR4 substrate, with a dielectric constant of e_r=4.6. The fabrication procedure requires only three masks on account of its simplicity and compatibility with PCB technology. The fabrication process employed readily available materials including, Aluminum foils and sheets, Glycidyl-ether-bisphenol-A novolac (SU-8), antimony-free photoacid ADEX dry film sheets; and organic solvents, Propylene Glycol Methyl Ether Acetate (PGMEA), and Cyclohexanone.

The fabrication and integration processes are illustrated in Fig. 2, and depict laser structured transmission lines on FR4 substrates, SU-8 patterned center dielectric layers, embossed

[1]Advanced Design System, 2016 ver., Keysight Technologies, SR., CA, 2016.

[2]ANSYS HFSS Electromagnetic Suite, Release 2014, Ansys Inc., Canonsburg, PA, 2014.

[3]Matlab,release R2016a, The MathWorks Inc., Natick, MA., 2016.

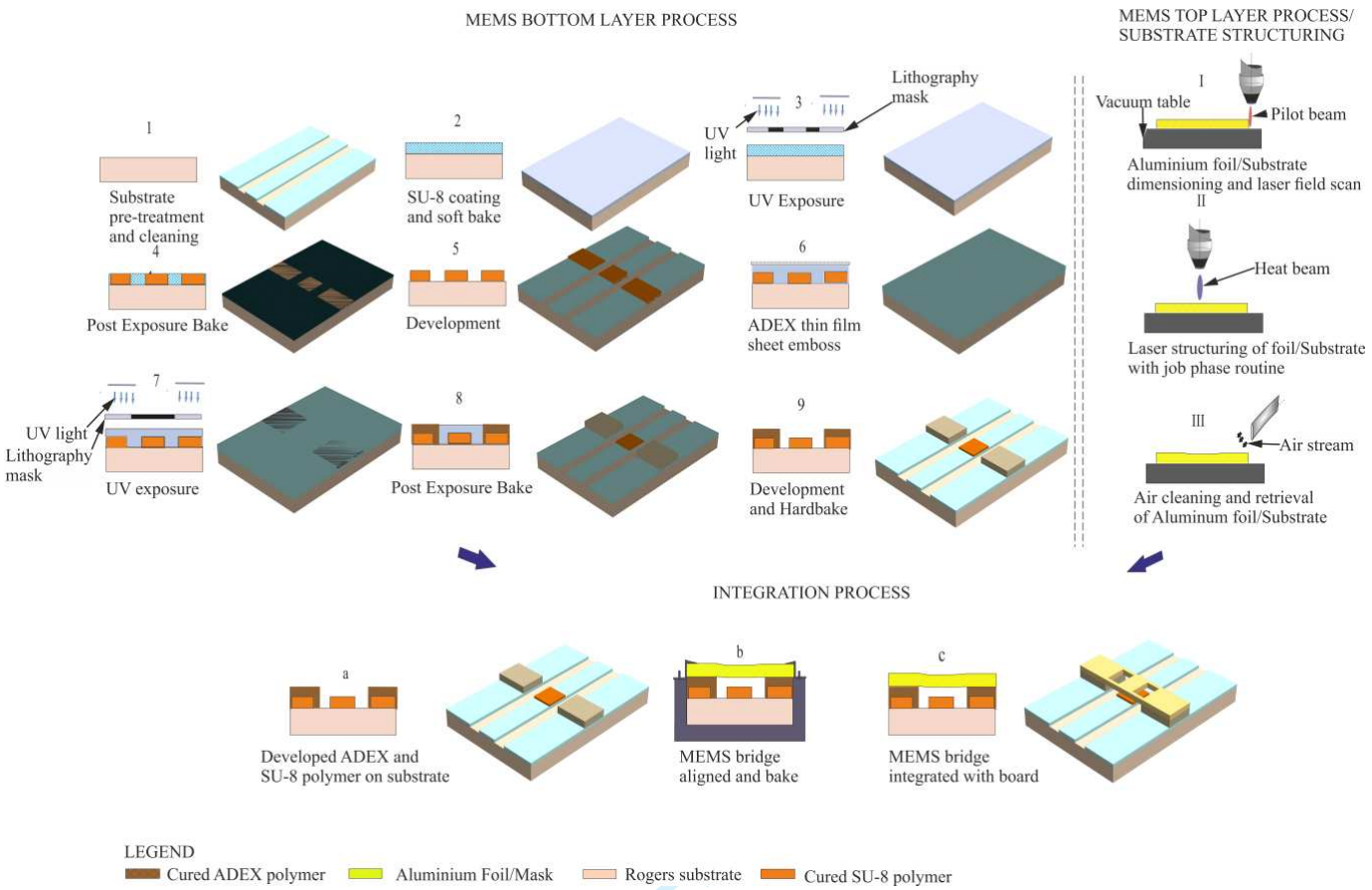

Fig. 2. Process flow for wet bench photolithography-ADEX hot film emboss and MEMS integration technique.

ADEX thin film polymers patterns for the bridge anchor support, and the final integration process of the MEMS membranes to the substrate. The reported process consists of an adaptation of wet bench fabrication processes with dry film embossing techniques, to implement multilayer microstructures with high aspect ratios, and adhesion properties with faster implementation cycles, when compared to standard cleanroom processes. Different sub-types of SU-8 possess varying viscosity allowing different coat thickness, which after curing and hard baking presents a near optically transparent layer with good mechanical and chemical resistive properties. Multilayer formulation of SU-8 structures has been widely reported, e.g. [18], based on a wet bench process with a Silicon substrate.

ADEX thin film sheets were developed by DJ DevCorp, and are dry thin film epoxy polymer sheets that are placed between two protective polyester film sheets (PET), with thickness ranging from 5 µm to 75 µm. It is a modification from an earlier dry thick film sheet epoxy line series, SUEX, with initial film thickness starting from 100 µm.

A combination of photolithography and hot embossing is used to pattern these polymers, with the cured coating presenting a uniform layer, possessing strong mechanical and excellent adhesive properties to metals and other polymers. Work reported in [19], and [20] provides an insight into multilayer applications of ADEX film sheets, and their robust mechanical and bonding properties. The combined application of both SU-8 photoresist and ADEX dry film sheets maximizes the benefits from both, with stable adhesion to the MEMS membrane offered in the latter, and a thin coat thickness obtained using the former.

We propose this process described in the Fig. 2, using micro-structuring of both Aluminum foil and copper cladded FR4 substrates, together with photolithography and thin film polymer emboss, to obtain a patterned substrate; and a final integration procedure for the MEMS component members.

A. Substrate layer

The low-cost implementation of the CPW transmission lines requires a subtractive methodology, compatible with commercial PCB etching methods. Various techniques considered in published literature [3, 15, 21] have established production with wet chemical batch etching and micro-fabrication as dominant methods. Recent work reported in [21] describes the fabrication of CPW lines from an Au layer deposited by thermal evaporation on a GaAs substrate, and using photolithography to define track width, anchor and actuation posts, following liftoff in an etch bath. In [15], an investigation into the properties of SU8 confirmed it as a cost effective photoresist for masks. This property was exploited in [3], to again fabricate CPW lines on a bare PCB substrate sputtered with a Ti/Cu layer, and transmission lines defined by photolithography. The processes employed in [3] and [21] are suited to a clean room environment, and are time-consuming and complicated, requiring the use of expensive equipment.

In line with our objectives, we adopted laser etching technique that made for fabrication of the transmission lines on copper cladded Duroid substrate boards, on account of its compatibility for PCBs. This procedure was also applied to realize micro-structuring of 14 µm thick Aluminum foils for the MEMS device membranes, and the 100 µm thick Aluminum sheets employed as lithography masks. Micro-structuring by laser, was adopted due to its relatively low cost, and short production time window, while still achieving design requirements.

The LPKF U3 Protolaser machine, with a laser beam resolution of 15 µm, made for ablation of desired copper regions on the substrate to achieve the transmission lines. The operation defining the copper surface rubout and structuring routine consists a sequence of steps indicated as follows. The first step in the fabrication sequence is to prepare the copper layer on the FR4 substrate for laser etching and structuring. PGEMA and dry air were employed as cleaning agents to remove dirt and surface impurities on the board. Thereafter the board start point and substrate thickness were scanned by a pilot diode beam, alongside an alignment of the board along the x, y, and z axis, through the positioning and travel by the beam, first at the origin of chuck and at target work piece. Adjustments in the alignment of the work piece was made possible by combination of servo motors in combination with vacuum suction pressure on the chuck.

A set of phase production parameters, which describe the laser and machine work excursion schedule, was set for optimized structuring of the CPW transmission lines. These parameters are related to the laser work fields supplied in the job allocation routine software, Circuit Master. This software also made for allocations of laser work field structures for both 100 µm Aluminum sheets, employed as the lithography masks, and the 14 µm foils used as the MEMS membranes. The fields include pre-heating of the target scan field in the pre-heat phase, an excursion of the heat laser beam along copper rub-out area in the contour phase, heating of the scanned target area in the heating phase.

The next step consists of the job extraction phase where a stream of high pressure air is fed on to the work and vacuum table to make for separation of debris from the structured transmission lines on the FR4 substrate.

To realize set goals, a range of optimized parameters consisting of frequency, power, jump time delay, speed and repeat cycles were derived. The optimal working pressure is for the routine developed is 6 bars. A summary of this process is indicated in the laser substrate structuring section of Fig. 2.

B. MEMS membrane layer

The MEMS top layer subsection shown in Fig. 2, describes the stages involved in the micro-structuring of 14 µm Aluminum foils by laser. Both MEMS switches and varactors movable membrane are fabricated using this technique, with a modification of the production field parameters of the LPKF U3 Protolaser machine indicated in section A. The laser beam frequency and repeat cycles were also modified to obtain the desired structure from the foils. The upper Aluminum MEMS members, varactor and switch bridges, fabricated using this technique are shown in Fig. 3A), and Fig. 3B) respectively. And are seen to consist of flexible suspensions, bridge, anchor termination points. They are suspended over the CPW transmission line as depicted in the microphotograph in Fig. 3.

C. MEMS dielectric and support layers

The MEMS devices to be integrated to the substrate require multilayer polymer deposits to make for the desired air gap, and a dielectric layer on the center conductor. The dominant trend consists of designating a polyimide layer as the sacrificial layer. Various processes for fabricating the sacrificial layer, with adhesion of the layers to substrate and membrane materials as governing concerns, have been reported in [1], and [23-25]. These processes include suiting deposition technologies, such as electroplating, chemical and vapor deposition, alongside matching etching techniques, including Ion Coupled Plasma (ICP) etching and Reactive Ion Etching (RIE). Improvements in the SU8 photolithography process were reported in [26], with exposure regulation and aperture channel control. Another method entails transferring laminated films of SU-8 as reported in [26], with a removable material to make for micro-channels. Multilayer SU-8 deposition requires a repeat of the polymer coating on the substrate and accompanying lithography curing procedure, mirroring the number of layers.

The procedure adopted to realize this layer is chosen to be a blend of photo-lithography and a hot emboss of the ADEX thin film epoxy on the substrate, for the switches and multi-layer SU-8 coating for the varactors. This adaptive process is aptly described as the wet bench-dry film press, with a transition between polymer depositions via spin coating, to embossing dry film polymer on the substrate. A description of this process would follow in this section, and has been optimized for both copper cladded FR4 substrate, and the MEMS membrane.

The process begins with a preparation of the substrate and structured transmission lines, through cleaning by Isopropanol (IPA), and pre-heating to allow for dehydration. Thereafter SU-8 2002 resist is spun on the substrate at 4000 rpm, ramped from 500 rpm with the Chemat KW-4A-CE spin coater, with excess beads trimmed after this deposition. The copper cladded surface of the substrate now coated with 1 µm layer of SU-8 2002, is soft baked at 95°C, and ramped from 65°C, prior to exposure, to reduce the viscous flow accompanying deposition of the resist. This process steadies the SU-8 coat which would also be in close contact with the mask in the curer, when it is exposed to Ultra-violet (UV) light. Curing is made possible by 365 nm wavelength UV light provided by the Chemat KW-4AC, with the chuck rotating at 6 rpm to make for uniform exposure. This process results in cross-linking of the SU-8 layer. The exposed substrate and SU-8 is baked at a stepped temperature of 65°C, and at 95°C. This process results in a polymerized layer of SU-8, with discernible patterns on the substrate. Development of the wafer is done in PGMEA, and with further cleaning in propanol. Additional baking of the substrate at 65°C and then 95°C is required to allow for complete curing of this initial posts and patterned center line dielectric SU-8 polymer layer.

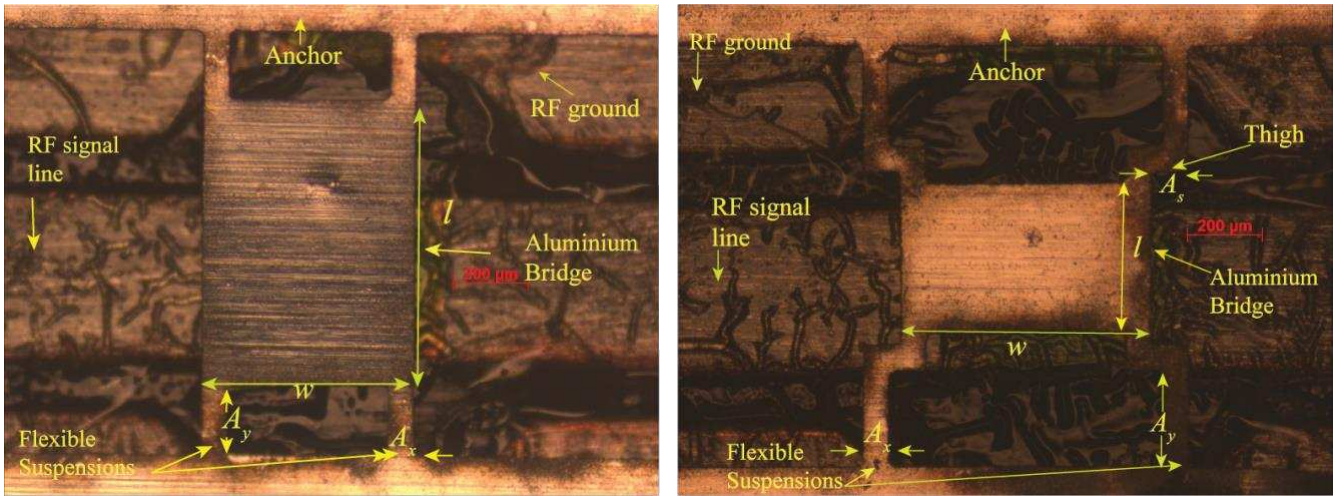

MEMS switch (a) MEMS varactor (b)

Fig. 3. Microphotograph of the MEMS Aluminum varactor

To make for patterning of the MEMS suspension anchor posts, an additional sacrificial coat of SU-8 2002 resist is spun on the wafer, thereafter the ADEX sheet is embossed on to the substrate at 65℃, by feeding both film and substrate into the SKY 335R6 laminator at 0.3 m/min. A thin uniform layer of the ADEX polymer is stamped onto the copper cladded substrate, with this process. The carrier Polyethylene terephthalate (PET) film is carefully peeled off the substrate leaving behind 5 um layers of the ADEX film polymer. Curing of this embossed polymer, is also provided by the Chemat KW-4AC UV. The wafer is later baked on an oven at 65℃, and stepped up to 85℃, to make for polymerization of the anchor post patterns, which would now be visible. The substrate is thereafter soaked and agitated in Cyclohexanone, to ensure development of the polymer. A summary of this process employed to realize the ADEX and SU-8 polymer patterns and posts is indicated in bottom layer section of process ensemble depicted in Fig. 2. The alignment accuracy achieved between the two dielectric layers, i.e. the SU-8 and ADEX layers, was found to be, on average, 69 µm. This accuracy is defined as the difference between the structures as designed and simulated and any misalignment after fabrication is complete.

The CPW transmission lines obtained from the rubout of the copper cladded FR4 board with the LPKF U3 machine, is now observed to be patterned with 1 µm dielectric layer of SU-8 2002 on the signal line, and as foundation for the 5 µm ADEX epoxy polymers deposits developed from dry film. This provides the required elevation, for the bridge anchors from the CPW ground plane. Measured dimensions of fabricated structures are shown in Table II.

TABLE II
MEASURED DIMENSIONS OF FABRICATED RF MEMS DEVICES

Symbol	MEMS device geometry	Switch (µm)	Varactor (µm)
l	Bridge length	772	414
w	Bridge width	567	685
A_x	Suspension width	86	84
A_y	Suspension length	127	129
d_o	Bridge height	6.2	2.3
t_d	Dielectric height	1.1	1.2

D. MEMS device integration process

With the ADEX support posts and SU-8 resist layers now developed, integration of the MEMS device follows. The process consists of an alignment of the Aluminum MEMS members with 2.48 mm diameter circular fiducials, positioned on both substrate and MEMS membranes. A holding fixture, composed of an Aluminum block, is milled with complimentary fiducial markers to provide accurate positioning of the substrate with the MEMS membranes. Alignment accuracy between the Aluminum sheet layer and the dielectric posts, using this method, was found to be, on average, 49.5 µm. The method used for determining this is the same as that for the alignment accuracy between the SU-8 and ADEX layers, described previously. Each member is lowered onto the alignment fixture, alongside the substrate by calipers in calibrated steps with observation through a microscope. Propanol, IPA, is used to rinse the wafer and the sacrificial layer of SU-8 2002, which consequently ensures air gap between the bridge and the transmission line. To ensure complete polymerization, in addition to making for a composite assembly, the substrate, MEMS bridge, and alignment fixture posts held in place by the aligner, is then hard baked at 150℃, ramped from 130℃ for two hours, to ensure all structures are set, in addition to furthering cross linking and ensuring the stability of the patterned polymers. Finally, the substrate, it is allowed to cool, and air dried to forestall the possibility of the MEMS bridges being pulled down by the surface tension of the any leftover fluids or moisture.

The integration process that made for the bonding of the MEMS membrane with the board, and patterned polymers is as depicted in the integration subsection of Fig. 2. The aligner fixture was milled from an Aluminum block, with a recess to make for accommodation of MEMS device assembly, and fiducial embossed fixture cover.

IV. Results and Discussion

The RF response of both MEMS switch and varactor was measured from 0.1-6 GHz by an E8316A PNA Network

Analyzer, connected via SMA cables to 500 µm pitch coplanar probes Cascade Microtech microprobes, ACP-GSG-500, mounted on a Cascade Microtech 9600 Thermal probe station. Monitoring of the DUT was by a combination of Olympus SZ-CTV 60 microscope and an AmScope 5MP USB Microscope Digital camera. The DUT was held in place by vacuum suction unto the chuck of the probe station. The effects of the probes and connected cables to the PNA were de-embedded by on wafer standard wideband SOLT calibration methods. Actuation of the devices was provided by a series termination comprising an Agilent 6811B power supply, a 1 MΩ resistor, and a bias-tee separating connected SMA cables from feeding direct DC power to the PNA, while allowing for RF measurements.

A. MEMS Switch

A comparison between the simulated and measured reflection coefficient $S_{11}$and transmission coefficient S_{21} of a typical RF MEMS switch fabricated using the process presented in this paper, is shown in Fig. 4 and Fig. 5, for the UP and DOWN, respectively. As shown in Fig. 4, the reflection coefficient of the 600 µm bridge width MEMS switch following the shunt loading of the CPW transmission line is measured at 2 GHz to be -19.6 dB, compared to a simulated value of -18.25 dB, for the UP state position. Also shown in Fig. 4, the transmission loss of this switch in the UP state from measurements at 2 GHz is -0.63 dB, compared to -0.25 dB from simulations. All simulation results were obtained from the commercial 3D EM software package Ansys HFSS.

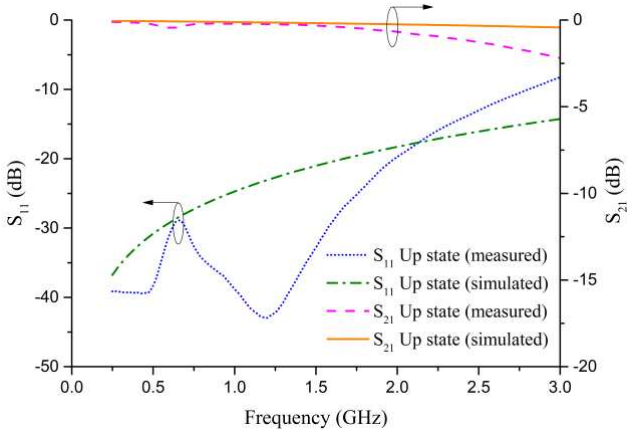

Fig. 4. MEMS Aluminum switch return and transmission loss UP state response.

In the DOWN state, the return loss of the switch from measurements at 2 GHz as indicated in Fig. 5, is -4.8 dB compared to -1.2 dB from simulations. The measured isolation of the switch, defined as $S_{21}^{DOWN} - S_{21}^{UP}$ at 2 GHz is -7.3 dB, while the simulation result is -7.6 dB.

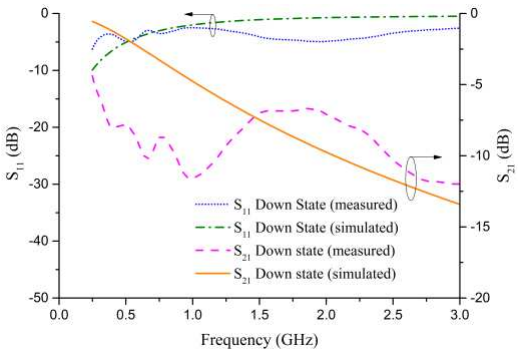

Fig. 5. MEMS Aluminum switch return and transmission loss DOWN state response.

B. MEMS Varactor

Similarly to the MEMS switch, the S_{11} and S_{21} of the varactor were also measured for both its states. For an actuation voltage of 15 V, the RF performance of the 700 µm bridge width RF MEMS varactor in the UP state and DOWN state is presented in Fig. 6 and Fig. 7, respectively. The measured return loss for the varactor in the UP state is measured to be -16.96 dB at 2.5 GHz versus a simulated value of -15.1 dB. A transmission loss of -0.91 dB, was obtained from measurements at 2.5 GHz, in this state, and -0.38 dB from simulations.

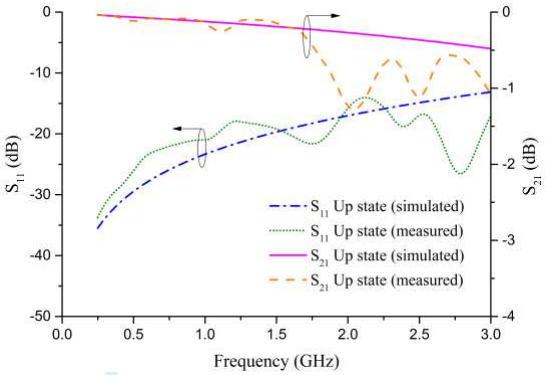

Fig. 6. MEMS Aluminum varactor return and transmission loss UP state response.

The DOWN state is given in Fig. 7, and in this case the measured return loss of the varactor is -16.35 dB at 2.5 GHz, compared to -11.3 dB from simulations. The insertion loss is similarly measured to be -1.21 dB compared to a simulated -0.61 dB at 2.5 GHz.

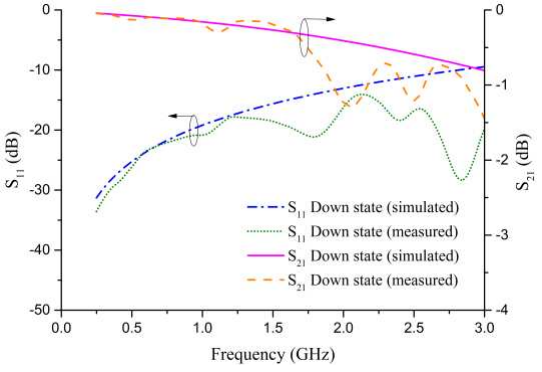

Fig. 7. MEMS Aluminum varactor return and transmission loss DOWN state response.

V. Conclusion

This paper presents the development of MEMS devices fabricated using laser micromachining techniques, wet bench processes and hot film emboss techniques on a FR4 substrate. The region of operation of these devices is up to 3 GHz. It is one of few reports that embarked on this set of combination processes aimed at providing cheaper fabrication solutions and with responses admissible for further development and improvement. It also includes design theory governing their operational principles, and an analysis of the RF response of the devices.

Two analog large area MEMS devices are designed with capacitance ratios to function as switch and varactor, while achieving desired RF responses. The states of these devices are electronically controlled by a bias voltage, 85 V for the switch, and 15 V for the varactor. These MEMS devices were fabricated with a high yield optimized wet bench and hot film press processes, and to the best of our knowledge the most cost-effective implementation methods for realizing MEMS devices.

A comparison of studied MEMS switch fabrication methods, their RF response and additional process type employed, relative to our work is presented in Table III.

TABLE III
COMPARISON OF KEY FACTORS OF MEMS DEVICES FABRICATION

Key factor	[2]	[4]	[3]	[5]	Our work
MEMs device type	Switch	Switch	Switch	Switch	Switch/Varactor
Membrane material	Gold/Titanium	Gold	Chromium/Gold	Gold/Chromium	Aluminum
Operating Frequency	DC - 3 GHz	2 GHz	6 GHz	5 GHz	2/2.5 GHz
Insertion loss OFF (dB)	-0.1	-0.25	-0.4	-36.6	-0.63/-0.91
Isolation ON (dB)	-27	-50	-16	-39.2	-7.3/-1.21
Return loss OFF (dB)	-20	N/A	-18	N/A	-19.6/-16.96
Return loss ON (dB)	N/A	N/A	-0.8	N/A	-4.8/-16.35
Actuation voltage (V)	0.5	12	37	93	85/15
Substrate type	Alumina	Silicon/Glass	TMM4	Silicon/RO4003	FR4
Fabrication techniques	Clean room (PECVD/Lithography/ Electroplating)	Clean room (PECVD/ RIE/ Wet etching)	Clean room (HDICP/Wet etching/ Electroplating)	Clean room (Evaporation/Lithography/ Sputtering)	Wet bench/ Hot film emboss/ Laser structuring
Fabrication complexity	Complicated	Complicated	Fairly complicated	Complicated	Simple
Overall costs (including materials)	High	High	Fairly high	Fairy high	Low

Acknowledgments

The authors would like to thank the EPSRC National Facility for Innovative Robotic Systems for the fabrication of some of the structures. Also, many thanks to Mr. Roland Clarke, for his assistance with measurements setup

References

[1] H. H Gatzen, V. Saile and J. Leuthold, Micro and Nano Fabrication Tools and Processes, 1st ed., Heidelberg, Germany: Springer, 2015, pp. 7-194.
[2] A. Attaran and R. Rashidzadeh, "Ultra low actuation voltage RF MEMS switch," Micro and Nano Systems Letters, vol. 3, Issue 1, pp. 1-4, Dec. 2015.
[3] M. W. B. Silva, S. E. Barbin and L. C. Kretly, "Fabrication and testing of RF-MEMS switches using PCB techniques," in IEEE MTT-S International Microwave and Optoelectronics Conf., Belem, Brazil, Nov. 2009, pp. 96-100.
[4] A. Kim, A. Kwon, H. Jeong, Y. Hong, S. Lee, I. Song and B. Ju, "A stiff and flat membrane operated DC contact type RF MEMS switch with low actuation voltage," Sensors and Actuators A: Physical, vol. 153, Issue 1, pp. 114-119, June 2009.
[5] K.S. Kiang, H.M.H. Chong, and M. Kraft, " A Novel Low Cost Spring-Less RF MES Switch Prototype," in Proceedings of 26th EuroSensors Conference, Linz Austria, Sept. 2010, pp. 1462-1465.
[6] Sami Franssila, Introduction to Microfabrication, 1st ed., W. Sussex, England: John Wiley, 2004, pp. 343-348.
[7] M. Maddela, R. Ramadoss and R. Lempkowski, "PCB MEMS-Based Tunable Coplanar Patch Antenna," in IEEE International Symposium on Industrial Electronics, Vigo, Spain, June 2007, pp. 3255-3260.
[8] H-P. Chang, J. Qian, B. A. Cetiner and F. D. Flaviis; M. Bachman, G. P. Li, "Design and Process Considerations for Fabricating RF MEMS Switches on Printed Circuit Boards," Journal of Microelectromechanical Systems, vol. 14, pp. 1311–1322, Dec. 2005.
[9] H-P. Chang, J. Qian, B. A. Cetiner and F. D. Flaviis; M. Bachman, G. P. Li, "RF MEMS switches fabricated on microwave-laminate printed circuit boards," IEEE Electron Device Letters, vol. 24, Issue. 4, pp. 227 – 229, April 2003.
[10] B. A. Cetiner, J. Y. Qian, H. P. Chang, M. Bachman, G. P. Li and F. D. Flaviis, "Microwave Laminate PCB Compatible RF MEMS Technology for Wireless Communication Systems," in IEEE Antennas and Propagation Society International Symp. Dig., Columbus, OH, June 2003, pp. 387-390.
[11] T. Homma, "Low dielectric constant materials and methods for interlayer dielectric films in ultralarge-scale integrated circuit multilevel interconnections," Materials Science and Engineering, vol. R23, pp. 243-285, Feb. 1998.
[12] W. Zheng, Q. Huang, X. Liao and F. Li, "RF MEMS Membrane Switches on GaAs Substrates for X-Band Applications," Journal of Microelectromechanical Systems, vol 14, no. 3, pp. 464-471, June 2005.
[13] S. P. Pacheco, L. P. B. Katehi, C. T. -C. Nguyen, "Design of Low Actuation Voltage RF MEMS Switch," in IEEE MTT-S International Microwave Symp. Dig., Boston, MA, August, 2000, pp. 165 – 168.
[14] N.S. Barker and G.M. Rebeiz, "Distributed MEMS True-Time Delay Phase Shifters and Wide-Band Switches," IEEE Trans. Microw. Theory Tech., vol. 46, no 11, pp. 1881-1890, Nov. 1998.
[15] G.M. Rebeiz, RF MEMS Theory, Design, and Technology, 1st ed., Hoboken, NJ, USA: John Wiley and Sons, 2003.
[16] G. K. Fedder, "Simulation of Microelectromechanical Systems," Ph.D. thesis, Elect. Eng. and Computer Science Graduate Division, University of California at Berkeley, Berkeley, CA, USA, 1994.
[17] Z. Zhou, Z. Wang, and L. Lin, Microsystems and Nanotechnology, 1st ed., Heidelberg, Germany: Springer, 2012, pp. 653-719.
[18] L. H, Despont, M. Fahrin, N. LaBianca, N. Renaud and P. Vettiger, "SU-8: A low-cost negative resist for MEMS," Journal of Micromechanics and Microengineering, vol 7, no 3, pp. 121-124, Sept. 1997.

[19] D. W. Johnson, J. Goettert, V. Singh and D. Yemane (2015 May). SUEX Dry Film Resist-A new Material for High Aspect Ratio Lithography., DJ Microlaminates, Sudbury, MA, [Online]. Available: https://djmicrolaminates.com/resources/white-papers-research-papers/.

[20] D. W. Johnson, J. Goettert, V. Singh and D. Yemane. (2012). Opportunities for SUEX dry laminate resist in microfluidic MEMS applications. LSU, Center for Advanced Microstructures & Devices., Baton Rouge, LA [Online]. Available: https://www.lsu.edu/camd/files/DJ_AR2012_SUEX_fluidic.pdf

[21] S. P. Pacheco, L. P. B. Katehi, C. T. -C. Nguyen, "Design of Low Actuation Voltage RF MEMS Switch," in IEEE MTT-S International Microwave Symp. Dig., Boston, MA, August, 2000, pp. 165 – 168.

[22] W. S. Timmer, Micromechanics and MEMS, Classic and Seminal papers to 1990, Piscataway, NJ, USA: IEEE Press, 1997, pp. 21-652.

[23] Y. Chen, H. Mao, Q. Tan, C. Xue, W. Ou, J. Liu, D. Chen, "Fabrication of polymide sacrificial layers with inclined sidewalls based on reactive ion etching," AIP advances, vol. 4, Issue 3, pp. 031328(1)-031328(7), Mar. 2014.

[24] K.J. Vinoy, G.J. Ananthasuresh, R. Pratap and S.B. Krupanighi, Micro and Smart Devices and Systems, 1st. ed., New Delhi, India, Springer, 2014. pp. 229-245.

[25] V. Linder, B. B. Gates, D. Ryan, B. A. Parviz, and G. M. Whitesides, "Water-soluble sacrificial layers for surface micromachining," Small, vol. 1, no. 7, pp. 730-736, Jul. 2005.

[26] Y.J.Chuang, F.G. Tseng, J.H. Cheng and W. K. Lin, "A novel fabrication method of embedded micro-channels by using SU-8 thick-film photoresists," Sensors and Actuators A: Physical, vol 103, pp. 64-69, Jan. 2003.